Ξ^--hypernuclear states in heavy nuclei

S. Tadokoro, H. Kobayashi, and Y. Akaishi
Institute for Nuclear Study, University of Tokyo, Tanashi, Tokyo 188, Japan
(Received 6 September 1994)

The possibility of observing heavy Ξ-hypernuclei by (K^-,K^+) reactions is investigated. Several narrow peaks are clearly seen in the K^+ spectrum of $^{208}\mathrm{Pb}(K^-,K^+)^{208}_{\Xi^-}\mathrm{Hg}$ reaction calculated by the Green's function method. They correspond to Ξ^- bound states with spin-stretched high angular momentum. The excitation of the Ξ^- bound states amounts to about 0.4 μb/sr MeV for the ^{208}Pb target in the case of 2 MeV detector resolution, which is considerably larger than that for the ^{12}C target. It is discussed whether or not the mass-number dependence of nucleus-Ξ potential depths is observed between $A=12$ and 208.

PACS number(s): 25.80.Nv, 21.80.+a, 21.60.−n

I. INTRODUCTION

Strangeness $S=-2$ hypernuclei would give important information concerning the ΞN and $\Lambda\Lambda$ interactions. Evidence for the formation of double-Λ hypernuclei is obtained from old emulsion experiments [1] and a recent experiment at KEK [2]. As for Ξ hypernuclei seven candidates from emulsion data are reviewed in a pioneering theoretical work by Dover and Gal [3]. Recently, there appear two events in the KEK emulsion experiment which may be attributed to the formation of Ξ-atoms and/or nuclei [4]. However, the supply of data on double-strangeness ($S=-2$) hypernuclei is still limited. At BNL, 1–2 GeV/c highly-intense and well-separated K^- beam becomes available and the $S=-2$ spectroscopy is now feasible by means of (K^-,K^+) reactions. We can expect to get experimental information on the nucleus-Ξ interaction by populating Ξ-hypernuclear states. Thus, a key problem at present would be the possible existence of bound Ξ-hypernuclei.

We investigate Ξ^--hypernuclear spectra from $^{208}\mathrm{Pb}(K^-,K^+)$ as well as $^{12}\mathrm{C}(K^-,K^+)$ by using the Green's function method [5]. In the case of ^{12}C Ikeda *et al.* discussed in detail the formation of Ξ^- states and calculated the transition rate from Ξ^- states to possible double-Λ states [6]. A remarkable feature they obtained is the narrowness of Ξ-state widths, which encourages the search for Ξ hypernuclei. Yamamoto has suggested that the depth of the nucleus-Ξ potential derived from the Nijmegen potential [7] has no saturation property but changes from about −12 MeV for $A=12$ to about −24 MeV for $A=208$ [8]. This is due to weak exchange force of the meson-theoretical ΞN potential. Thus, the mass-number dependence of nucleus-Ξ potential depth is an interesting problem in relation to the nature of ΞN interaction. In order to know whether the mass-number dependence really exists or not, the (K^-,K^+) experiment should be performed not only on light-nucleus target but also on heavy-nucleus target. Because core-excited states densely distribute in the heavy-target case, the reaction is required to have a selective population mechanism. We will show that the $^{208}\mathrm{Pb}(K^-,K^+)$ reaction with an incident momentum 1.65 GeV/c excites selectively Ξ^- bound states with spin-stretched high angular momentum. We propose an experimental search for some prominent Ξ^- peaks in ^{208}Pb.

In Sec. II we explain the Green's function method. The nucleus-Ξ potentials employed are discussed in Sec. III. The Ξ^--hypernuclear spectrum from $^{208}\mathrm{Pb}(K^-,K^+)$ is given in Sec. IV and compared with that from $^{12}\mathrm{C}(K^-,K^+)$. Summary and conclusions are given in Sec.V.

II. GREEN'S FUNCTION METHOD

The double-differential cross section for the (K^-,K^+) reaction is given within the distorted-wave impulse approximation (DWIA) as

$$\frac{d^2\sigma}{dE_{K^+}d\Omega_{K^+}}=\beta\left[\frac{d\sigma}{d\Omega_{K^+}}\right]^{(\mathrm{el})}S(E)\ , \tag{1}$$

where β is a kinematical factor, $[d\sigma/d\Omega_{K^+}]^{(\mathrm{el})}$ is the Fermi-averaged differential cross section for the elementary process $K^-+p\to K^++\Xi^-$ and $S(E)$ is the strength function of a hypernuclear system. The kinematical factor β is defined by

$$\beta=\left\{1+\frac{E^{(2)}_{K^+}}{E^{(2)}_{\Xi}}\;\frac{p^{(2)}_{K^+}-p_{K^-}\cos\theta_{K^+}}{p^{(2)}_{K^+}}\right\}\frac{p_{K^+}E_{K^+}}{p^{(2)}_{K^+}E^{(2)}_{K^+}}, \tag{2}$$

where $E^{(2)}_{K^+}$ $(p^{(2)}_{K^+})$ is total energy (momentum) of K^+ in the laboratory system determined by the free K^-N two-body kinematics at the incident momentum p_{K^-}. It is noted that β is not constant but proportional to $p_{K^+}E_{K^+}$. The strength function $S(E)$ is obtained by the Green's function method [5],

$$S(E)=-\frac{1}{\pi}\mathrm{Im}\sum_{\alpha\alpha'}\int d\mathbf{r}\,d\mathbf{r}'f_\alpha(\mathbf{r})G_{\alpha\alpha'}(E;\mathbf{r},\mathbf{r}')f_\alpha(\mathbf{r}'), \tag{3}$$

$$f_\alpha(\mathbf{r})=\chi^{(-)*}(\mathbf{p}_{K^+},M_C/M_{\mathrm{HY}}\mathbf{r})\chi^{(+)}(\mathbf{p}_{K^-},M_C/M_{\mathrm{HY}}\mathbf{r})\times\langle\alpha|\psi_N(\mathbf{r})|i\rangle, \tag{4}$$

where kets $|i\rangle$ and $|\alpha\rangle$ are states of the target and of a core nucleus, respectively and $\psi_{N(Y)}$ is the annihilation operator of $N(Y)$. Recoil effects are taken into account through the factor $M_C/M_{\rm HY}$ in Eq. (4) [9]. Here $G_{\alpha\alpha'}(E;\mathbf{r},\mathbf{r}')$ is Green's function for the hyperon interacting with the core nucleus.

$$G_{\alpha\alpha'}(E;\mathbf{r},\mathbf{r}') = \langle\alpha|\psi_Y(\mathbf{r})\frac{1}{E-H+i\eta/2}\psi_Y^\dagger(\mathbf{r}')|\alpha'\rangle, \quad (5)$$

with

$$H = T_{\rm nucl-\Xi} + U_{\rm nucl-\Xi}. \quad (6)$$

If $U_{\rm nucl-\Xi}$ is taken to be a single-particle optical potential, Green's function becomes diagonal with respect to core-nucleus states $|\alpha\rangle$. We can take into account spreading widths of proton-hole states (nuclear core states) and the energy resolution of a detector by putting a finite value into η in Eq. (5).

The distortion of meson waves is calculated in the eikonal approximation as

$$\chi^{(+)}(\mathbf{p}_{K^-},\mathbf{r}) = \exp\left[i\mathbf{p}_{K^-}\cdot\mathbf{r} - iv_{K^-}^{-1}\int_{-\infty}^{z_-} U_{K^-}(\mathbf{b}_-,z')dz'\right], \quad (7)$$

$$\chi^{(-)*}(\mathbf{p}_{K^+},\mathbf{r}) = \exp\left[-i\mathbf{p}_{K^+}\cdot\mathbf{r} - iv_{K^+}^{-1}\int_{z_+}^{\infty} U_{K^+}(\mathbf{b}_+,z')dz'\right], \quad (8)$$

$$z_- = \hat{\mathbf{p}}_{K^-}\cdot\mathbf{r}, \quad z_+ = \hat{\mathbf{p}}_{K^+}\cdot\mathbf{r}, \quad (9)$$

where $v_{K^\pm}$ is the velocity of the meson and $\mathbf{b}_-$ ($\mathbf{b}_+$) is the component of $\mathbf{r}$ perpendicular to $\mathbf{p}_{K^-}$ ($\mathbf{p}_{K^+}$). The meson-nucleus optical potential U_m (m stands for K^- or K^+) is given by

$$U_m(\mathbf{r}) = -i\tfrac{v_m}{2}\bar{\sigma}_{mN}\rho(\mathbf{r}), \quad (10)$$

$$\bar{\sigma}_{mN} = \sigma_{mN}^{\rm tot}(1-i\bar{\alpha}_{mN}), \quad \bar{\alpha}_{mN} = {\rm Re}\bar{f}(0)/{\rm Im}\bar{f}(0), \quad (11)$$

where $\sigma_{mN}^{\rm tot}$ is the isospin-averaged total meson-nucleon cross section and $\bar{f}(0)$ is the isospin-averaged forward elementary amplitude. We neglect the effect of $\bar{\alpha}_{mN}$ because the differential cross section is rather insensitive to it [10], and use the following meson-nucleon total cross sections [11]:

$$\sigma_{K^-p}^{\rm tot} = 32.5 \text{ mb}, \quad \sigma_{K^-n}^{\rm tot} = 25.5 \text{ mb},$$
$$\sigma_{K^+p}^{\rm tot} = 19.6 \text{ mb}, \quad \sigma_{K^+n}^{\rm tot} = 20.1 \text{ mb}, \quad (12)$$

which correspond to the case of an incident momentum p_{K^-}=1.65 GeV/c.

Straightforward angular momentum algebra gives partial-wave decomposition of $S(E)$:

$$S(E) = \sum_{JM}\sum_{l_Y,j_Y}\sum_{n_N,l_N,j_N}\sum_{l'_Y,j'_Y}\sum_{n'_N,l'_N,j'_N}\sqrt{(2j_N+1)(2j'_N+1)}$$
$$\times(j_N\tfrac{1}{2}J0|j_Y\tfrac{1}{2})\tfrac{1}{2}(1+(-1)^{l_N+l_Y+J})(j'_N\tfrac{1}{2}J0|j'_Y\tfrac{1}{2})\tfrac{1}{2}(1+(-1)^{l'_N+l'_Y+J})$$
$$\times S^{JM}_{(l_Yj_Y,n_Nl_Nj_N),(l'_Yj'_Y,n'_Nl'_Nj'_N)}(E), \quad (13)$$

$$S^{JM}_{(l_Yj_Y,n_Nl_Nj_N),(l'_Yj'_Y,n'_Nl'_Nj'_N)}(E) = -\tfrac{1}{\pi}{\rm Im}\int dr\int dr' r^2r'^2\tilde{j}_{JM}(p_{K^-},p_{K^+},\theta_{K^+};r)^*\phi_{n_Nl_Nj_N}(r)$$
$$\times G^J_{(l_Yj_Y,n_Nl_Nj_N),(l'_Yj'_Y,n'_Nl'_Nj'_N)}(E;r,r')\tilde{j}_{JM}(p_{K^-},p_{K^+},\theta_{K^+};r')\phi_{n'_Nl'_Nj'_N}(r'), \quad (14)$$

where the function $\tilde{j}_{JM}(p_{K^-},p_{K^+},\theta_{K^+};r)$ is defined by

$$\chi^{(-)*}(\mathbf{p}_{K^+},M_C/M_{\rm HY}\mathbf{r})\chi^{(+)}(\mathbf{p}_{K^-},M_C/M_{\rm HY}\mathbf{r}) = \sum_{J=0}^{\infty}\sum_{M=-J}^{M=J}\tilde{j}_{JM}(p_{K^-},p_{K^+},\theta_{K^+};r)Y_J^M(\hat{\mathbf{r}}), \quad (15)$$

$\phi_{n_Nl_Nj_N}(r)$ is a radial-part wave function of the proton which absorbs the incident meson and J is the total spin of the hypernucleus. In the case of forward K^+ production θ_{K^+}=0°, Eq. (13) and Eq. (14) are further reduced to

$$S(E) = \textstyle\sum_J\sum_{l_Y,j_Y}\sum_{n_N,l_N,j_N}\sum_{l'_Y,j'_Y}\sum_{n'_N,l'_N,j'_N}[W]S^J_{(l_Yj_Y,n_Nl_Nj_N),(l'_Yj'_Y,n'_Nl'_Nj'_N)}(E), \quad (16)$$

$$[W] = (2J+1)\sqrt{(2j_N+1)(2j'_N+1)}(j_N\tfrac{1}{2}J0|j_Y\tfrac{1}{2})\tfrac{1}{2}(1+(-1)^{l_N+l_Y+J})(j'_N\tfrac{1}{2}J0|j'_Y\tfrac{1}{2})\tfrac{1}{2}(1+(-1)^{l'_N+l'_Y+J}), \quad (17)$$

$$S^J_{(l_Yj_Y,n_Nl_Nj_N),(l'_Yj'_Y,n'_Nl'_Nj'_N)}(E) = -\tfrac{1}{\pi}{\rm Im}\int dr\int dr' r^2r'^2\tilde{j}_J(p_{K^-},p_{K^+};r)^*\phi_{n_Nl_Nj_N}(r)$$
$$\times G^J_{(l_Yj_Y,n_Nl_Nj_N),(l'_Yj'_Y,n'_Nl'_Nj'_N)}(E;r,r')\tilde{j}_J(p_{K^-},p_{K^+};r')\phi_{n'_Nl'_Nj'_N}(r'), \quad (18)$$

where we use the relation

$$\tilde{j}_{JM}(p_{K^-},p_{K^+},\theta_{K^+}=0°;r) = i^J\sqrt{4\pi(2J+1)}\tilde{j}_J(p_{K^-},p_{K^+};r)\delta_{M0}. \quad (19)$$

We neglect couplings between $(n_N l_N j_N)$ and $(n'_N l'_N j'_N)[\neq(n_N l_N j_N)]$, and between $(l_Y j_Y)$ and $(l'_Y j'_Y)[\neq (l_Y j_Y)]$ by adopting single-particle potentials.

The differential cross section to a definite hypernuclear bound state is obtained by integrating Eq. (1) on small energy interval suitably chosen, and is expressed as

$$\frac{d\sigma}{d\Omega_{K^+}} = \alpha \left[\frac{d\sigma}{d\Omega_{K^+}}\right]^{(\mathrm{el})} Z^{\mathrm{eff}}, \tag{20}$$

$$\alpha = \left(\frac{p_{K^+}}{p^{(2)}_{K^+}}\right)^2 \frac{p^{(2)}_{K^+}/E^{(2)}_{K^+} + (p^{(2)}_{K^+} - p_{K^-}\cos\theta_{K^+})/E^{(2)}_{\Xi}}{p_{K^+}/E_{K^+} + (p_{K^+} - p_{K^-}\cos\theta_{K^+})/E_{\mathrm{HY}}}, \tag{21}$$

where Z^{eff} is the effective proton number of the exclusive reaction. One should avoid confusions between α and β, and between Z^{eff} and $S(E)$.

III. NUCLEUS-Ξ POTENTIAL

Dover and Gal [3] made theoretical analyses of old emulsion data attributed to (K^-, K^+) Ξ-hypernuclear productions [12] and extracted nucleus-Ξ potentials of Woods-Saxon type;

$$U_{\mathrm{nucl}-\Xi} = \frac{V_0 + iW_0}{1 + \exp\{(r-R)/a\}} \tag{22}$$

with V_0 = -24±4 MeV (real-part strength), $R = 1.1A^{1/3}$ fm and a = 0.65 fm.

We assume the nucleus-Ξ^- potential of Woods-Saxon form with the same values of range and diffuseness parameters as the above. The imaginary-part strength is taken to be $W_0 = -1$ MeV. This imaginary part, together with the real part $V_0 = -24$ MeV, gives level widths of 1.2 MeV for $1s$ state and of 0.5 MeV for $1p$ state in the Ξ^--^{11}B system. These widths are in good agreement with the $\Xi^- p \to \Lambda\Lambda$ conversion widths obtained from the Nijmegen model-D potential [7] by Ikeda *et al.* [6]. We examine also a stronger conversion case of $W_0 = -3$ MeV to know how results are sensitive to the imaginary potential.

The real-part strength V_0 is assumed to be -24 MeV for ^{208}Pb. We, however, employ $V_0 = -16$ MeV in addition to -24 MeV for ^{12}C. Reasons why we investigate the shallow potential case are the followings. Yamamoto has suggested that the depth of the nucleus-Ξ potential derived from the Nijmegen interaction has no saturation property but depends on the mass number of the core nucleus [8]. This property is attributed to the fact that no single meson carries double strangeness and therefore the exchange force is weak between Ξ and N. Aoki *et al.* observed the twin Λ-hyperfragment production via Ξ^- capture by the emulsion-counter hybrid experiment at KEK [4]. The energy of the stopped Ξ^- on ^{12}C is estimated to be -0.54 ± 0.20 MeV, which deviates from the finite-size Coulomb levels, -0.97 MeV for $1s$, -0.28 MeV for $2p$ and -0.26 MeV for $2s$. The $V_0 = -16$ MeV potential, when it is added to the Coulomb potential, shifts down the $2p$ state to -0.56 MeV, giving a plausible (but not unique) explanation for the stopped Ξ^- energy.

IV. Ξ^--HYPERNUCLEAR SPECTRA FROM (K^-, K^+) REACTIONS

Spectra for ^{12}C(K^-, K^+) and ^{208}Pb(K^-, K^+) reactions are calculated at forward-angle $\theta_{K^+} = 0°$ with an incident momentum p_{K^-}=1.65 GeV/c. We adopt $[d\sigma/d\Omega_{K^+}]^{(\mathrm{el})}$= 35 μb/sr [13]. In the calculation two proton-hole states $1p^{-1}_{3/2}$ and $1s^{-1}_{1/2}$ are included for the ^{12}C case and six proton-hole states $3s^{-1}_{1/2}$, $2d^{-1}_{3/2}$, $1h^{-1}_{11/2}$, $2d^{-1}_{5/2}$, $1g^{-1}_{7/2}$ and $1g^{-1}_{9/2}$ for the ^{208}Pb case. Proton-hole wave functions are calculated by using the Woods-Saxon potential with geometrical parameters of r_0=1.27 fm and a=0.67 fm. We employ strength parameters of V_0 = -61 MeV, V_{LS}=22 MeV. Hypernuclear spectra do not strongly depend on the detail of proton-hole wave functions, especially in the Ξ^- bound state region. Spreading widths of the proton-hole states are taken from ^{12}C$(p, 2p)$ [14] and ^{208}Pb$(e, e'p)$ [15] experiments. We assume ΔE = 2 MeV as the energy resolution of a spectrometer. Results are shown in Figs. 1 and 2. The quasifree production of Ξ^- gets much stronger than the bound-state population, because of large momentum transfer 0.5 GeV/c which is about two times as large as the Fermi momentum in a nucleus. It is noted that all the deep-hole states sizably contribute to the continuum spectrum.

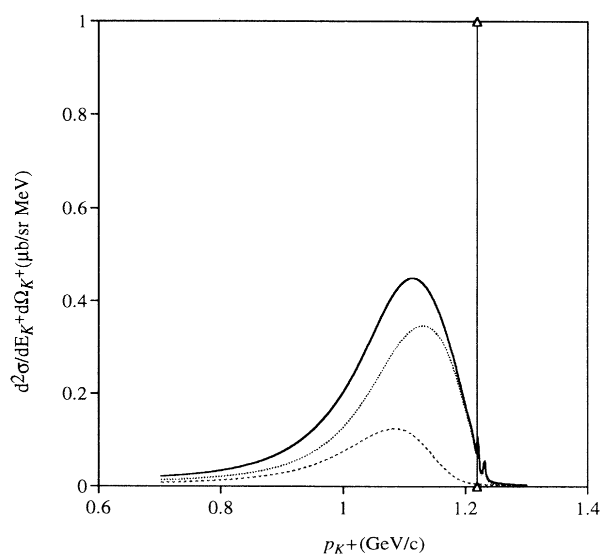

FIG. 1. The Ξ^--hypernuclear spectrum from ^{12}C(K^-, K^+) for p_{K^-}=1.65 GeV/c and θ_{K^+} = 0°. The threshold of Ξ^- and the core nucleus (ground state) is denoted by the vertical line. The full curve represents the total double-differential cross section. The dotted and dashed curves are for the contributions from proton hole states $1p^{-1}_{3/2}$ and $1s^{-1}_{1/2}$, respectively.

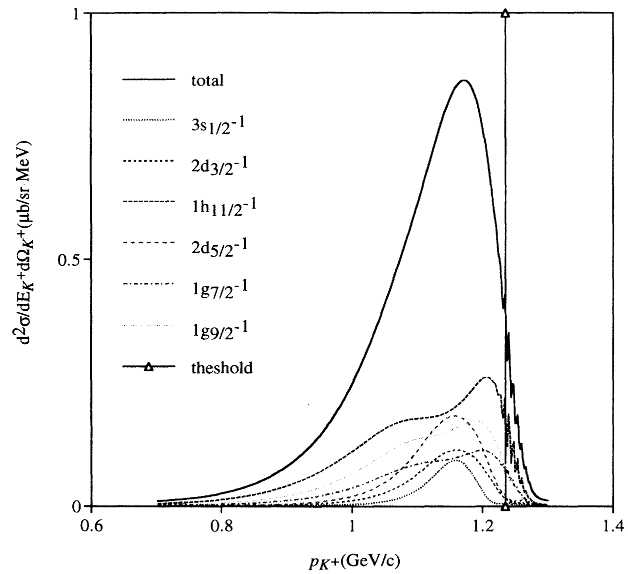

FIG. 2. The same spectrum from ^{208}Pb(K^-,K^+) for p_{K^-}=1.65 GeV/c and $\theta_{K^+} = 0°$. See also the caption of Fig. 1.

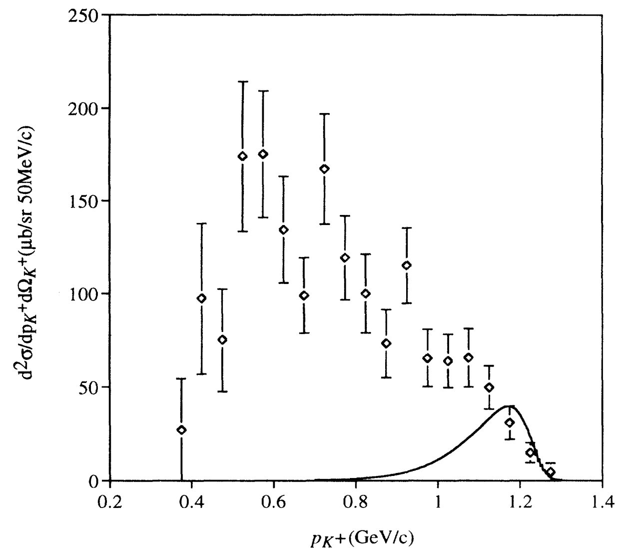

FIG. 4. The same as Fig. 3 but for the ^{208}Pb target case.

In Figs. 3 and 4 the calculations are compared with experimental data obtained at KEK by Iijima *et al.* [13]. The experimental data are averaged between $\theta_{K^+} = 1.7°$ and 13.6°. However, we show the result at $\theta_{K^+} = 0°$ because one at 13.6° is almost same. The magnitudes of the cross sections are fairly reproduced by our calculation in the Ξ^- quasifree production region. Since energies of Ξ^- are very high in the quasifree region, for example about 100 MeV at the quasifree peak, Ξ^- hardly feels the influence of the nucleus-Ξ^- potential. Therefore, even if we change parameters of nucleus-Ξ^- potential, the spectra in the quasifree region are almost unchanged.

A. ^{12}C (K^-,K^+) $^{12}_{\Xi^-}$Be

Let us discuss in detail the spectra in the bound-state region of Ξ^-. Figure 5 shows the spectrum for

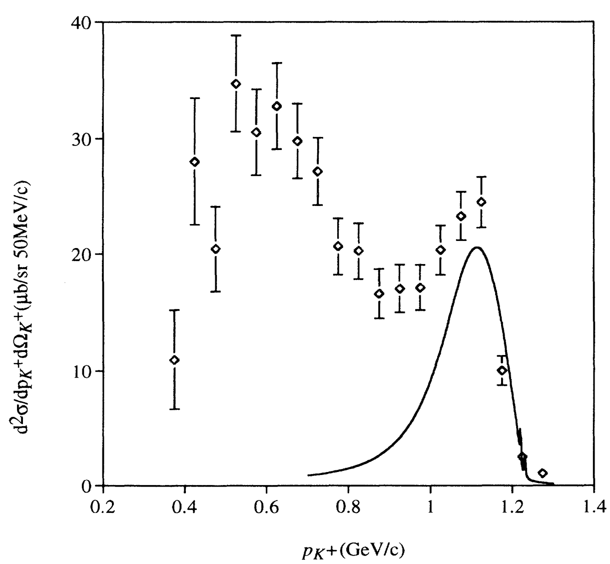

FIG. 3. Comparison between our calculated spectrum ($\theta_{K^+} = 0°$) for ^{12}C target and the KEK experimental data taken from Ref. [13]. The experimental spectrum is averaged between $\theta_{K^+} = 1.7°$ and 13.6°.

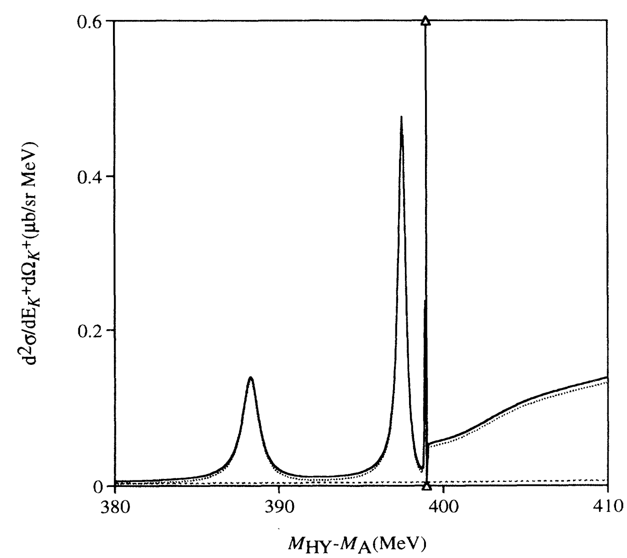

FIG. 5. The hypernuclear spectrum for ^{12}C target in the bound-state region as a function of $M_{\rm HY} - M_A$, where $M_{\rm A}$ and $M_{\rm HY}$ are target and hypernuclear masses, respectively. The spectrum is calculated with $V_0 = -24$ MeV and $W_0 = -1$ MeV. Energy resolution is taken to be 0 MeV.

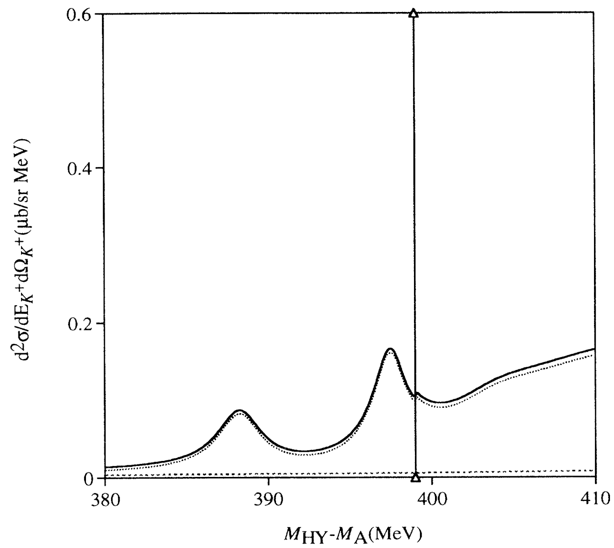

FIG. 6. The same as Fig. 5 but it is smeared with $\Delta E = 2$ MeV.

the ^{12}C target calculated with $V_0 = -24$ MeV and $W_0 = -1$ MeV, where the energy resolution is taken to be zero in order to compare it with the previous result by Ikeda *et al.* [6]. Two separated peaks appear below the $\Xi^- +\ ^{11}$B threshold at 399 MeV. The lower and upper peaks correspond to the excitation of hypernuclear states $[p1p_{3/2}^{-1} \otimes \Xi s_{1/2}]^{J=1}$ and $[p1p_{3/2}^{-1} \otimes \Xi p]^{J=0,2}$, of which decay widths are 1.2 MeV and 0.5 MeV, respectively. The widths are in good agreement with what Ikeda *et al.* obtained from the Nijmegen model-D potential. In the quasifree production region, however, our spectrum

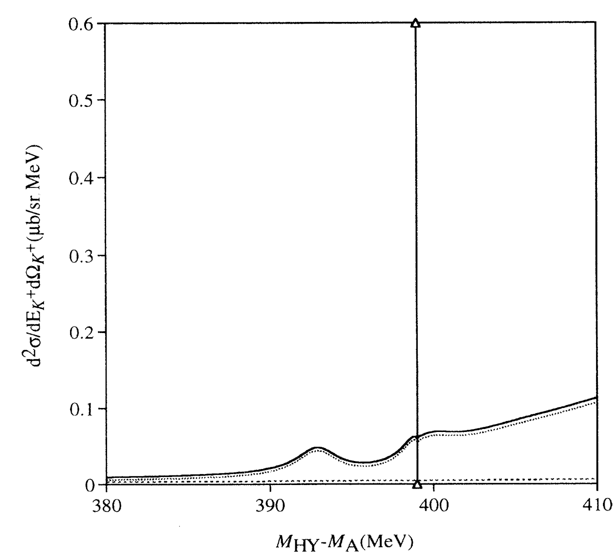

FIG. 7. The same as Fig. 6 but it is calculated with $V_0 = -16$ MeV.

is smooth, while their spectrum is rugged even though there is no resonance. This indicates that the Green's function method is easier to get a good description of the continuum spectrum than the Kapur-Peierls method used by them. We introduce into the spectrum the effect of energy resolution of a spectrometer. The result with 2 MeV smearing is shown in Fig. 6. The heights of two peaks at M_{HY}-$M_A \sim 387$ MeV and 398 MeV become about 0.09 and 0.17 μb/sr MeV, respectively. The effective proton numbers are estimated to be 0.012 and 0.017.

There is a possibility that the depth of the nucleus-Ξ potential depends on the mass number of core nucleus, as stated in Secs. I and III. Figure 7 shows the spectrum when the shallow potential of $V_0 = -16$ MeV is used. In this case there remains only one peak which corresponds to the $[p1p_{3/2}^{-1} \otimes \Xi s_{1/2}]^{J=1}$ configuration.

B. ^{208}Pb (K^-, K^+) $^{208}_{\Xi^-}$Hg

Figures 8(a) and 8(b) show the spectra for the ^{208}Pb target calculated with $V_0 = -24$ MeV and $W_0 = -1$ MeV in the cases of energy resolution $\Delta E = 0$ MeV and of $\Delta E = 2$ MeV, respectively. In the spectra we can see a series of Ξ^- bound-state peaks at M_{HY}-$M_A \sim 358$, 362, 368, 374, 381, and 387 MeV below the $\Xi^- +\ ^{207}$Tl threshold at 391 MeV. The prominent ones at 374, 381, and 387 MeV correspond to the excitation of spin-stretched states $[p1h_{11/2}^{-1} \otimes \Xi h_{9/2}]^{J=10}$, $[p1h_{11/2}^{-1} \otimes \Xi i_{11/2}]^{J=11}$ and $[p1h_{11/2}^{-1} \otimes \Xi j_{13/2}]^{J=12}$, respectively, as explained later. The selective excitation of spin-stretched states in the high momentum transfer reaction was pointed out many years ago by Dover *et al.* [10]. Hole states with small angular momentum such as $3s_{1/2}^{-1}$, $2d_{3/2}^{-1}$, $2d_{5/2}^{-1}$ are hardly excited in the Ξ^- bound-state region by the (K^-, K^+) reaction with large momentum transfer, though they give sizable contributions to the spectrum in the Ξ^- quasifree production region. Furthermore the second largest-l hole states, $1g_{9/2}^{-1}$ and $1g_{7/2}^{-1}$, show no sharp-peak structures because of their broad spreading widths [15]. Thus, the spectrum of ^{208}Pb(K^-, K^+) has the structure determined dominantly by the excitation of $p1h_{11/2}^{-1} \otimes \Xi^-$ hypernuclear states.

Let us discuss the structure of the prominent peaks in detail. Figure 9 shows the excitation spectra of the hypernuclear states with the configuration $p1h_{11/2}^{-1} \otimes \Xi$. A selection rule

$$l_p + l_\Xi + J = \text{even} \tag{23}$$

follows from the factor $[1 + (-1)^{l_N + l_Y + J}]/2$ in Eq. (17) which comes from the matrix element $\langle (l_Y 1/2) j_Y || \mathbf{Y}^J || (l_N 1/2) j_N \rangle$. For example, although $\Xi h_{9/2}$, $\Xi h_{11/2}$ and $\Xi j_{13/2}$ can contribute to the J=10 hypernuclear state, the first one dominates the others by forming a spin-stretched state together with $p1h_{11/2}^{-1}$. Similarly, $\Xi j_{13/2}$ and $\Xi j_{15/2}$ are relevant in the case of the J=12 state, and the former gives the main component again forming a spin-stretched state. Figure 10 compares contributions from ls splitting partners. One of them is so weakly excited due to angular-momentum coupling coefficients of Eq. (17) that the ls splitting of Ξ^- cannot be observed but, fortunately, does not destroy the peak structures in Fig. 8. Thus, it is known that the J=12 peak almost purely consists of the $[p1h_{11/2}^{-1} \otimes \Xi j_{13/2}]^{J=12}$ state.

It is noted that Ξ^- single-particle bound states exist at least up to l_Ξ=7 with the assistance of the Coulomb attraction between Ξ^- and ^{207}Tl. Figure 11(a) shows Ξ^- density distributions together with the net potential which is a sum of strong, Coulomb and centrifugal poten-

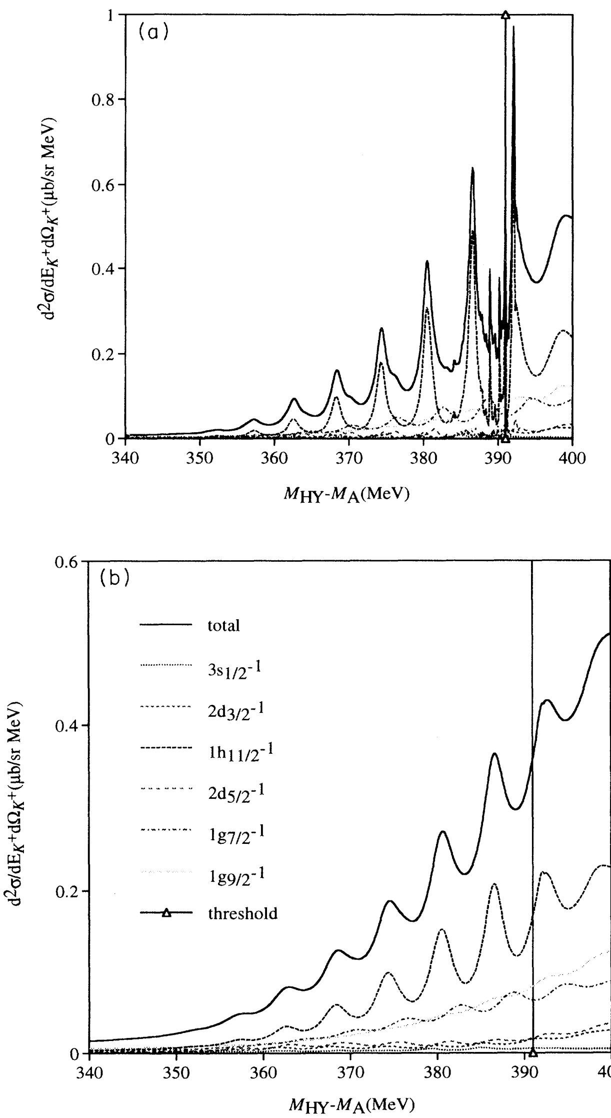

FIG. 8. The spectrum from ^{208}Pb(K^-, K^+) for $p_{K^-} = 1.65$ GeV/c and $\theta_{K^+} = 0°$ calculated with $V_0 = -24$ MeV and $W_0 = -1$ MeV. (a) The case of resolution $\Delta E = 0$ MeV. (b) The case of $\Delta E = 2$ MeV.

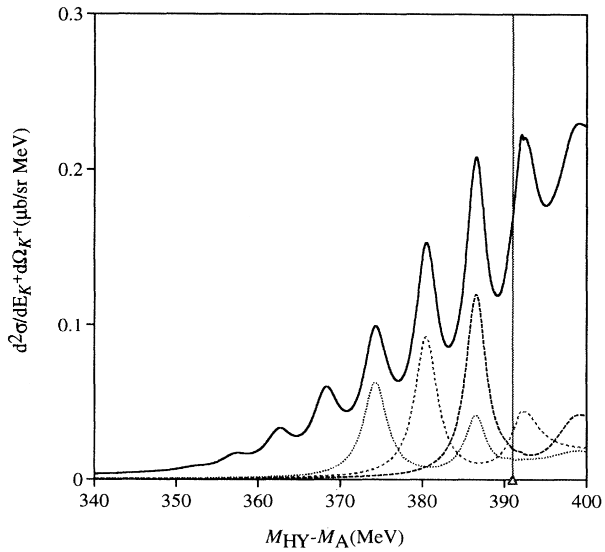

FIG. 9. The total excitation spectrum of hypernuclear states with the $p1h_{11/2}^{-1} \otimes \Xi^-$ configuration (solid curve), and the contributions from spin-stretched hypernuclear states $[p1h_{11/2}^{-1} \otimes \Xi h_{9/2}]^{J=10}$ (dotted curve), $[p1h_{11/2}^{-1} \otimes \Xi i_{11/2}]^{J=11}$ (dashed curve) and $[p1h_{11/2}^{-1} \otimes \Xi j_{13/2}]^{J=12}$ (long-dashed curve).

tials. The dotted line is for the l_Ξ=7 state with energy -5.8 MeV and the dot-dashed line is for a l_Ξ=0 state with energy -5.4 MeV. We can see that the l_Ξ=7 state is well confined in the nuclear surface region by the centrifugal potential and is essentially different from the l_Ξ=0 Coulomb atomic state. As a result, the final $\Xi j_{13/2}$ state has a remarkably good overlap with the initial $\mathrm{p}1h_{11/2}$

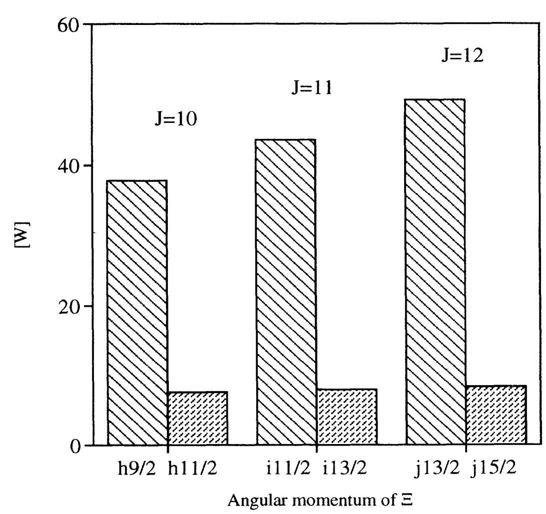

FIG. 10. Weight factors of ls splitting partners for the same J.

state shown in Fig. 11(b). Furthermore partial waves $\tilde{j}_{J=12}(p_{K^-}, p_{K^+}; r)$ in Eq. (18) is peaked at $r \sim 6$ fm due to the large momentum transfer. Therefore the J=12 peak gets prominent. Thus the centrifugal force plays an essential role in strongly exciting the spin-stretched high-J states. It was discussed by Bandō and Motoba that pairs with nodeless single-particle wave functions acquire a particularly strong population in the case of the (π^+, K^+) reaction [16]. The present result provides another typical example of their statement with a physical explanation.

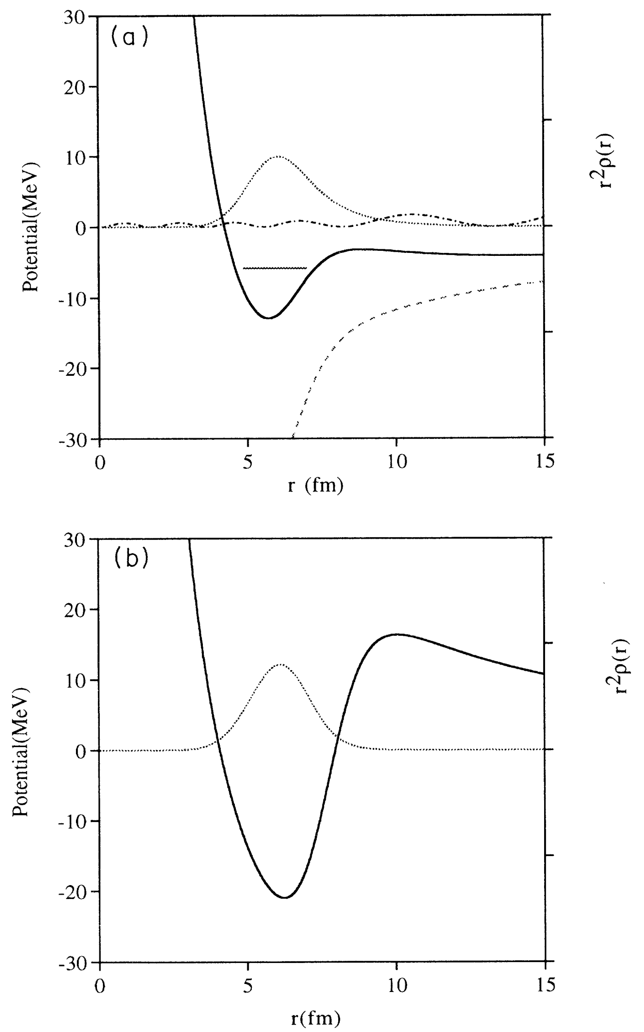

FIG. 11. Probability distributions and potentials for Ξ^- and p. (a) The Ξ^- case: The solid curve is for the net potential of strong, Coulomb and centrifugal ones with l_Ξ=7. The dashed curve is for the potential without the centrifugal one. The dotted and dot-dashed curves are for density distributions of the $\Xi 1j$ state with energy -5.8 MeV and of the $\Xi 6s$ state with energy -5.4 MeV, respectively. (b) The proton case: The solid curve is for the net potential with l=5. The dotted curve is for the density distribution of the $p1h_{11/2}$ state.

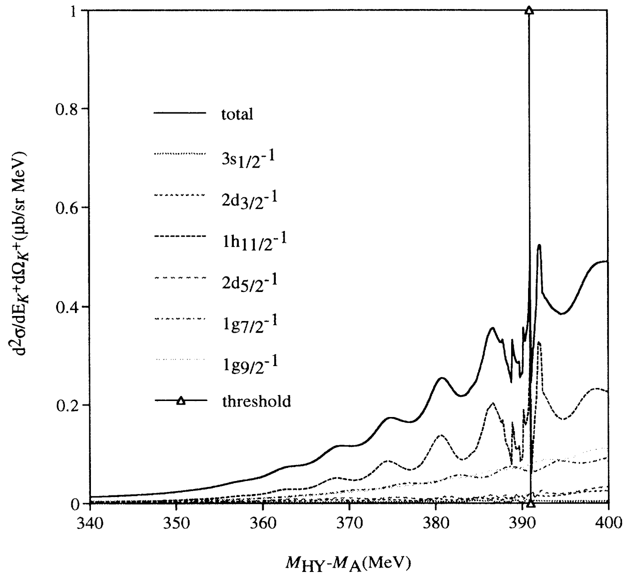

FIG. 12. The same spectrum as Fig. 8(a) but calculated with $W_0 = -3$ MeV and $V_0 = -24$ MeV. Energy resolution is $\Delta E = 0$ MeV.

We examine the effect of the imaginary strength of the nucleus-Ξ^- potential. Figure 12 shows the spectrum which is calculated with $W_0 = -3$ MeV and $V_0 = -24$ MeV in the case of zero resolution. The peaks at $M_{HY} - M_A \sim 374$, 381, and 387 MeV, which are clearly seen in Fig. 8, become broad but still remain. Many sharp peaks around the Ξ^- threshold are due to the excitation of Ξ^- atomic states. If a very high resolution spectrometer would become available, several hypernuclear peaks can be observed even in the strong imaginary case of $W_0 = -3$ MeV which gives a width of 6 MeV in nuclear matter. On the contrary, we could consider the case of a weaker strength than $W_0 = -1$ MeV for high-J Ξ states. Such possibility of width suppression will be investigated elsewhere.

Finally it should be mentioned that the $p1h_{11/2}^{-1}$ state of ^{207}Tl is not dispersed as seen from the ^{208}Pb$(e, e'p)$ experiment [15]. This may provide a justification of our treatment of $p1h_{11/2}^{-1} \otimes \Xi$ states based on the single-particle models. In sum, the characteristics of the (K^-, K^+) reaction makes it possible to observe some isolated peaks due to the excitation of Ξ^--hypernuclear bound states even in the case of ^{208}Pb. The most prominent peak at $M_{HY} - M_A \sim 387$ MeV in Fig. 8(b) has a height of 0.4 μb/sr MeV and an effective proton number of 0.024.

V. SUMMARY AND CONCLUSIONS

The K^+ spectra for ^{12}C and ^{208}Pb(K^-, K^+) reactions are calculated at forward-angle $\theta_{K^+} = 0°$ with p_{K^-}=1.65 GeV/c by using the Green's function method. The nucleus-Ξ potential is assumed to be of Woods-

Saxon form with complex strengths, $V_0 = -24$ MeV and $W_0 = -1$ MeV. The calculated spectra are folded with an energy resolution of $\Delta E = 2$ MeV.

In the spectrum of ^{12}C there appear two narrow peaks which correspond to the $[p1p_{3/2}^{-1} \otimes \Xi s_{1/2}]^{J=1}$ and $[p1p_{3/2}^{-1} \otimes \Xi p]^{J=0,2}$ hypernuclear states, as has been shown by Ikeda *et al.* [6]. The double differential cross sections to the lower and upper states are estimated to be 0.09 and 0.17 μb/sr MeV, respectively, when a spectrometer of ΔE=2MeV resolution is used. Since it is suggested that the nucleus-Ξ potential depth is shallower for ^{12}C than for ^{208}Pb, the spectrum is also calculated with $V_0 = -16$ MeV for ^{12}C. In this case, there remains only one peak in the spectrum.

In the spectrum of ^{208}Pb several well-separated peaks are observed in spite of many possible excitations, as seen from our main result Fig. 8(b). The peaks have the spin-stretched high-J structure, and the most prominent one is the $[p1h_{11/2}^{-1} \otimes \Xi j_{13/2}]^{J=12}$ state bound by about 6 MeV below the Ξ^- threshold. The (K^-, K^+) reaction populates selectively high angular-momentum states with no node. The configuration $p1h_{11/2}^{-1} \otimes \Xi$ essentially determines the shape of the spectrum from the ^{208}Pb(K^-, K^+) reaction. The high-l_Ξ single-particle state can be bound with the assistance of strong Coulomb attraction between Ξ^- and ^{207}Tl. The centrifugal force also plays an essential role. Since the force confines Ξ^- in the nuclear surface region, the Ξ^- single-particle state is not an atomic but a nuclear state. Because of a remarkably good overlap between the initial $p1h_{11/2}$ and the final $\Xi j_{13/2}$ wave functions, the J=12 hypernuclear state is strongly excited with a double-differential cross section of 0.4 μb/sr MeV and an effective proton number of 0.024.

It is investigated how the spectrum changes if a stronger imaginary strength of $W_0 = -3$ MeV is adopted. The peaks in ^{208}Pb become broad and are hardly distinguished from each other with a ΔE=2 MeV resolution detector. However, if we could use a high-resolution spectrometer, some of individual peaks can be separated out even in this strong imaginary case.

By carrying out (K^-, K^+) experiments on both light ^{12}C and heavy ^{208}Pb targets, we can expect to clarify whether or not the mass-number dependence of the nucleus-Ξ potential depth exists. An experimental observation of Ξ^- states in ^{208}Pb is awaited.

ACKNOWLEDGMENTS

The authors would like to thank Professor Y. Yamamoto, Professor T. Fukuda, and Professor S.W. Hong for valuable discussions. This work was supported by the Grants-in-Aid for Scientific Research of the Japanese Ministry of Education, No. 06640377.

[1] M. Danysz *et al.*, Phys. Rev. Lett **11**, 29 (1963); D.J. Prowse, *ibid.* **17**, 782 (1966).
[2] S. Aoki *et al.*, Prog. Theor. Phys. **85**, 1287 (1991).
[3] C.B. Dover and A. Gal, Ann. Phys. (NY) **146**, 309 (1983).
[4] S. Aoki *et al.*, Prog. Theor. Phys. **89**, 493 (1993).
[5] O. Morimatsu and K. Yazaki, Nucl. Phys. **A435**, 727 (1985); **A483**, 493 (1988).
[6] K. Ikeda, T. Fukuda, T. Motoba, M. Takahashi, and Y. Yamamoto, Prog. Theor. Phys. **91**, 747 (1994).
[7] M.M. Nagels, T.A. Rijken, and J.J. de Swart, Phys. Rev. **D 12**, 744 (1975); **15**, 2547 (1977); **20**, 1633 (1979).
[8] Y. Yamamoto (private communication).
[9] E.H. Auerbach, A.J. Balitz, C.B. Dover, A. Gal, S.H. Kahana, L. Ludeking, and D.J. Millener, Ann. Phys. (NY) **148**, 381 (1983).
[10] C.B. Dover, L. Ludeking, and G.E. Walker, Phys. Rev. **C 22**, 2073 (1980).
[11] Particle Data Group, Phys. Rev. D **45**, 1 (1992).
[12] D.H. Wilkinson, S.J. St. Lorant, D.K. Robinson, and S. Lokanathan, Phys. Rev. Lett. **3**, 397 (1959); A. Bechdolff, G. Baumann, J.P. Gerber, and P. Cüer, Phys. Lett. **26B**, 174 (1968).
[13] T. Iijima *et al.*, Nucl. Phys. **A546**, 588 (1992).
[14] H. Tyrén, S. Kullander, O. Sundberg, R. Ramachandran, and P. Isacsson, Nucl. Phys. **79**, 321 (1966).
[15] A.E.L. Dieperink and P.K.A. de Witt Huberts, Annu. Rev. Nucl. Part. Sci. **40**, 239 (1990).
[16] H. Bandō and T. Motoba, Prog. Theor. Phys. **76**, 1321 (1986).